Tree-based Reconstruction of Ecological Network from Abundance Data

Raphaëlle Momal¹*, Stéphane Robin¹, Christophe Ambroise²

1: UMR MIA-Paris, AgroParisTech, INRA, Université Paris-Saclay, 75005 Paris, France

2: Laboratoire de Mathématiques et Modélisation d'Évry, 23 bvd de France, Évry, France

May 29, 2022

Summary

- 1. The behavior of ecological systems mainly relies on the interactions between the species it involves. In many situations, these interactions are not observed and have to be inferred from species abundance data. To be relevant, any reconstruction network methodology needs to handle count data and to account for possible environmental effects. It also needs to distinguish between direct and indirect interactions and graphical models provide a convenient framework for this purpose.
- 2. We introduce a generic statistical model for network reconstruction based on abundance data. The model includes fixed effects to account for environmental covariates and sampling efforts, and correlated random effects to encode species interactions. The inferred network is obtained by averaging over all possible tree-shaped (and therefore sparse) networks, in a computationally efficient manner. An output of the procedure is the probability for each edge to be part of the underlying network.
- 3. A simulation study shows that the proposed methodology compares well with state-of-theart approaches, even when the underlying network strongly differs from a tree. The analysis of two data sets highlights the influence of covariates on the inferred network.
- 4. Accounting for covariates is critical to avoid spurious edges. The proposed approach could be extended to perform network comparison or to look for missing species.

Key-words: abundance data, covariates adjustment, ecological networks, EM algorithm, graphical models, matrix tree theorem, Poisson log-Normal model, species interactions

1 Introduction

Abundance data is often analysed using species distribution model (Elith and Leathwick, 2009), where species are traditionally considered as disconnected entities. However there is a growing awareness of biotic interactions being crucial components of biodiversity and relevant descriptors of an ecosystem (Jordano, 2016; Valiente-Banuet et al., 2015). Observing species interactions is a laborious task which restricts them to certain categories (e.g. trophic, pollination) while many other mutualistic and/or antagonistic interactions may be key in the system organization (e.g. competition for resources, communication, shelter sharing, etc). Model-based methods can help reconstruct such biotic interactions from observations collected on every species in a series of samples. Such interactions can be conveniently represented by ecological networks, which

^{*}Electronic address: raphaelle.momal@agroparistech.fr; Corresponding author

have been increasingly studied and used in recent years for describing and understanding living systems in ecology (Poisot et al., 2016), microbiology (Faust and Raes, 2012) or genomics (Evans et al., 2016). This work focuses on ecological network reconstruction based on observed species abundance data.

Network inference from species abundance measures is a notoriously difficult problem (Ulrich and Gotelli, 2010). First, it has to account for the data specificities. Abundance data consists of counts that may spread over a wide range of values, and often result from sampling efforts that may be sample-specific or species-specific, making them difficult to compare. Furthermore, indirect statistical association may be observed between two species and would interfere with interpretation. They can occur either because two species are both affected by the same environmental variations, or interacting with the same third species (Morueta-Holme et al., 2016). Therefore, any approach aiming at reconstructing ecological networks needs to account both for sampling efforts and covariates describing the environment, as well as distinguish between direct and indirect associations among species.

Graphical models (see Lauritzen, 1996, for a general introduction) provide a formal probabilistic framework to describe the dependency structure between a set of variables. In a graphical model, two variables are connected if they are directly dependent, whereas two variables are unconnected if they are independent conditionally on all others. In the present setting, the variables of interest are the species respective abundances. Fig. 1 illustrates the concept of conditional dependencies and spurious edges with four toy graphical models. In (a), the network is connected so all species are interdependent. However, species 1 does not have direct interactions with species 3 and 4: it is independent from them conditionally on species 2. In (b), the network is disconnected: species 4 is independent from all others. (c) corresponds to the case where two species (1) and (1) are not in direct interaction, and affected by the variations of the same environmental covariate (1) Lastly, (1) displays the graphical model when (1) is not accounted for: a 'spurious' edge appears between the two species. In that sense, graphical models enjoy all the desirable properties to represent interactions between species in an interpretable manner.

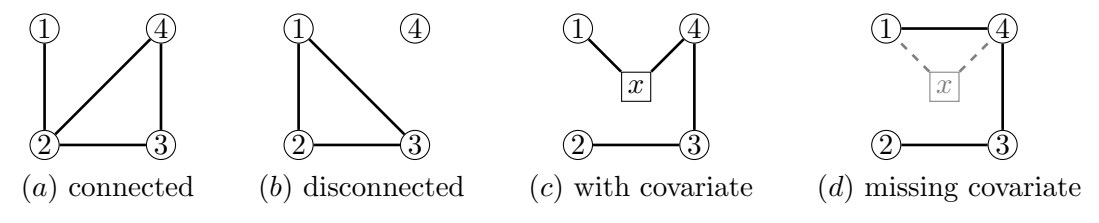


Figure 1: Examples of graphical models.

Network reconstruction is impeded by the huge number of possible graphs for a given set of species. It increases super-exponentially with the number of species, making the inference very hard from a combinatorial point of view. To reduce the search space, a common and reasonable assumption is that a relatively small fraction of species pairs are in direct interaction: the network is sparse. In the case of continuous observations, one of the most popular approach is the graphical lasso (glasso, Friedman et al., 2008) which takes advantage of the properties of Gaussian graphical models (GGM) to efficiently infer a sparse network. As the Gaussian setting is not suitable for count data, an alternative is to transform them into continuous data and then apply the glasso. This is the spirit of methods like gCoda (Fang et al., 2017) and SPIEC-EASI (Kurtz et al., 2015), which use slightly different transformations. Additionally, counts can not be seen as absolute measurements of the respective species abundances, as they typically depend on the sampling effort which may vary from one site to another. gCoda and SPIEC-EASI account for the sampling effort by treating counts as compositional data, which does not model the randomness due to sampling in an explicit manner. Alternatively, the sampling effort can

be taken into account via an offset term, which is the representation we adopt.

The Poisson log-Normal model (PLN, Aitchison and Ho, 1989) provides a convenient framework to deal with multivariate count data, without resorting to any transformation. The PLN model is a special instance of latent space models, which received attention recently in community ecology (see Warton et al., 2015). The PLN model combines generalized linear models to account for covariates and offsets, and a Gaussian latent structure to describe the species interactions. In that sense, it can be seen as a multivariate mixed model, in which correlated random effects encode the dependency between the species abundances. The MInt method (Biswas et al., 2016) uses the PLN model and combines it with the glasso to perform network inference.

The present approach adopts the PLN model but resorts to tree-shaped models to foster sparsity instead. Tree-structured graphical models have been early considered by Chow and Liu (1968), both to enforce sparsity and to take advantage of efficient algebraic tools. The tree assumption means that the associated network does not have any loop (see Fig. 2 (top)). This is obviously much too stringent in many contexts, and Meilă and Jaakkola (2006) and Kirshner (2008) later suggested to approximate the joint distribution of a set of variables by averaging over all possible tree-structured graphical models. As shown in Fig. 2 (bottom), the result of such an averaging procedure may not be a tree. Importantly, averaging over all tree-shaped models still benefits of efficient algebraic tools.

We introduce the method EMtree, which combines two (variational) EM algorithms to estimate the model parameters. Importantly, our approach provides the probability for each possible edge to be part of the interaction network. We evaluate our approach on both synthetic and ecological data sets. An R package implementing EMtree is available on GitHub https://github.com/Rmomal/EMtree.

2 Material and methods

2.1 Model

Let us first introduce the data at hand. We assume that p species have been observed in n sites and we denote Y_{ij} the abundance of species j in site i. The abundances are gathered in the $n \times p$ matrix \mathbf{Y} . We denote by \mathbf{Y}_i the ith row of matrix \mathbf{Y} , which corresponds to the abundance vector collected in site i. We further assume that a vector of covariates \mathbf{x}_i has been measured in each site i and that all covariates are gathered in the $n \times d$ matrix \mathbf{X} . The sites are supposed independent.

Our aim is to decipher the dependency structure between the p species, accounting for the effect of the environmental covariates encoded in \mathbf{X} . As explained above, ignoring environmental covariates is more than likely to result in spurious edges. Correcting for such confounding effects is necessary to make network inference meaningful.

Mixed model. To distinguish between covariates effects and species interactions, we consider a mixed model which states that each abundance Y_{ij} has a (conditional) Poisson distribution

$$Y_{ij} \sim \mathcal{P}\left(\exp(\mathbf{x}_i^{\mathsf{T}}\boldsymbol{\theta}_j + o_{ij} + Z_{ij})\right).$$
 (1)

In model (1), o_{ij} is the sample-specific and species-specific offset which accounts for the sampling effort. θ_j is the vector of fixed regression coefficients measuring the effect of each covariate on species j abundance. The regression part is similar to a general linear model as used in niche modelling (see e.g. Austin, 2007). Z_{ij} is a random effect, hence a random vector $\mathbf{Z}_i = (Z_{i1}, \ldots Z_{ip})$ (with dependent coordinates) is associated with each abundance vector \mathbf{Y}_i . This

random term precisely accounts for the species interactions that are not due to environmental fluctuations. Distribution (1) is over-dispersed as the Poisson parameter is itself random, which suits ecological modelling as over-dispersion with respect to the Poisson distribution is often observed in abundance data (Richards, 2008).

We now describe the distribution of the latent vector \mathbf{Z}_i . To this aim, we adopt a version of Kirshner's model (Kirshner, 2008), which states that a spanning tree T is first drawn with probability

$$p(T) = \prod_{(j,k)\in T} \beta_{jk}/B,\tag{2}$$

where $(j,k) \in T$ means that the edge connecting species j and k is part of the tree T and where B is a normalizing constant. Each edge weight β_{jk} controls the probability for the edge (j,k) to be in the interaction network.

Then for each site i, a vector \mathbf{Z}_i is drawn independently with conditional Gaussian distribution $(\mathbf{Z}_i \mid T) \sim \mathcal{N}(0, \Sigma_T)$, where the subscript T means that the distribution of \mathbf{Z}_i is faithful to T. When T is a spanning tree, this faithfulness simply means this distribution can be factorized on the nodes and edges of T as follows (see Kirshner, 2008):

$$p(\mathbf{Z}_i \mid T) = \prod_{j=1}^p p(Z_{ij} \mid T) \prod_{(j,k) \in T} \psi_{jk}(\mathbf{Z}_i), \tag{3}$$

where $\psi_{jk}(\mathbf{Z}_i)$ does not depend on T. This factorization means that each edge of T corresponds to a species pair in direct interaction; all other pairs are conditionally independent. Experiments are independent, and in the sequel we consider the product of all $p(\mathbf{Z}_i)$ and use the simpler notation $\psi_{jk} = \prod_i \psi_{jk}(\mathbf{Z}_i)$ instead.

According to (2), each \mathbf{Z}_i has a Gaussian distribution conditional on the tree T, so its marginal is a mixture of Gaussian distributions: $\mathbf{Z}_i \sim \sum_{T \in \mathcal{T}} p(T) \mathcal{N}(0, \Sigma_T)$, where \mathcal{T} is the set of all spanning trees. As a consequence, the joint distribution of the \mathbf{Z}_i is modeled by a mixture of distributions with tree-shaped dependency structure.

Besides, for all trees including the edge (j, k), the estimate of the covariance term between the coordinates j and k is the same (see Lauritzen, 1996; Schwaller et al., 2015). As a consequence, we may define a global covariance matrix Σ , filled with covariances that are each common to spanning trees containing a same edge. Each Σ_T is then built by extracting from Σ the covariances corresponding to the edges of T.

2.2 Inference with EMtree

We now describe how to infer the model parameters. We gather the edges weights $(\beta_{jk})_{jk}$ into the $p \times p$ matrix $\boldsymbol{\beta}$ and the vectors of regression coefficients into a $d \times p$ matrix $\boldsymbol{\theta}$. The $p \times p$ matrix $\boldsymbol{\Sigma}$ contains the variances and covariances between the coordinates of each latent vector \mathbf{Z}_i . Hence, the set of parameters to be inferred is $(\boldsymbol{\beta}, \boldsymbol{\Sigma}, \boldsymbol{\theta})$.

Likelihood. The model described above is an incomplete data model, as it involves two hidden layers: the random tree T and the latent Gaussian vectors \mathbf{Z}_i . The most classical approach to achieve maximum likelihood inference in this context is to use the EM algorithm (Dempster et al., 1977). Rather than the likelihood of the observed data $p(\mathbf{Y})$, the EM algorithm deals with the often more tractable likelihood $p(T, \mathbf{Z}, \mathbf{Y})$ of the complete data. It can be decomposed as

$$p_{\beta, \Sigma, \theta}(T, \mathbf{Z}, \mathbf{Y}) = p_{\beta}(T) \times p_{\Sigma}(\mathbf{Z} \mid T) \times p_{\theta}(\mathbf{Y} \mid \mathbf{Z}), \tag{4}$$

where the subscripts indicate on which parameter each distribution depends.

Observe that the dependency structure between the species is only involved in the first two terms, whereas the third term only depends on the regression coefficients $\boldsymbol{\theta}$. We take advantage of this decomposition to propose a two-stage estimation algorithm. The first stage deals with the observed layer $p_{\boldsymbol{\theta}}(\mathbf{Y} \mid \mathbf{Z})$, the second with the two hidden layers $p_{\boldsymbol{\beta}}(T)$ and $p_{\boldsymbol{\Sigma}}(\mathbf{Z} \mid T)$. The network inference itself takes place in the second step.

Inference in the observed layer. The variational EM (VEM) algorithm that provides an estimate of the regression coefficients matrix $\boldsymbol{\theta}$ is described in Appendix A.1. It also provides the (approximate) conditional means $\mathbb{E}(Z_{ij}|\mathbf{Y}_i)$, variances $\mathbb{V}(Z_{ij}|\mathbf{Y}_i)$ and covariances $\mathbb{C}\text{ov}(Z_{ij}, Z_{ik}|\mathbf{Y}_i)$ required for the inference in the hidden layer. As a consequence, this first step estimates $\widehat{\boldsymbol{\theta}}$ and $\widehat{\boldsymbol{\Sigma}}$.

Inference in the hidden layer. The second step is dedicated to the estimation of β . The EM algorithm actually deals with the conditional expectation of the complete log-likelihood, namely $\mathbb{E}(\log p_{\beta,\Sigma,\theta}(T,\mathbf{Z},\mathbf{Y}) \mid \mathbf{Y})$. As shown in Appendix A.2, this reduces to

$$\mathbb{E}\left(\log p_{\beta, \mathbf{\Sigma}, \boldsymbol{\theta}}(T, \mathbf{Z}, \mathbf{Y}) \mid \mathbf{Y}\right) \simeq \sum_{1 \le j < k \le p} P_{jk} \log \left(\beta_{jk} \widehat{\psi}_{jk}\right) - \log B + \text{cst}$$
 (5)

where $\widehat{\psi}_{jk}$ is the estimate of ψ_{jk} defined in (3), and the 'cst' term depends on $\boldsymbol{\theta}$ and $\boldsymbol{\Sigma}$ but not on $\boldsymbol{\beta}$. P_{jk} is the approximate conditional probability (given the data) for the edge (j,k) to be part of the network: $P_{jk} \simeq \mathbb{P}\{(j,k) \in T \mid Y\}$. It is also shown in Appendix A.2 that $\widehat{\psi}_{jk} = (1 - \widehat{\rho}_{jk}^2)^{-n/2}$, where the estimated correlation $\widehat{\rho}_{jk}$ depends on the conditional mean, variance and covariances of the Z_{ij} 's provided by the first step. (5) is maximized via an EM algorithm iterating the calculation of the P_{jk} and the maximization with respect to the β_{jk} :

E step: Computing the P_{jk} with tree averaging. The conditional probability of an edge is simply the sum of the conditional probabilities of the trees that contain this edge. Hence, computing P_{jk} amounts to averaging over all spanning trees. Fig. 2 illustrates the principle of tree averaging for a toy network with p = 4 nodes. Here, five arbitrary spanning trees T_1 to T_5 (among the $p^{p-2} = 16$ spanning trees) are displayed, with their respective conditional probability $p(T \mid Y)$. The edge (1,3) has a high conditional probability P_{13} because it is part of likely trees such as T_3 and T_4 , whereas P_{23} is small because the edge (2,3) is only part of unlikely trees (e.g. T_1, T_2).

As the number of possible trees is super-exponential in p, averaging cannot be carried out in a naive way. However, thanks to the Matrix Tree theorem (Chaiken and Kleitman, 1978, recalled as Theorem 1 in Appendix A.3) this is achievable at the cost of a determinant calculus (with complexity $O(p^3)$). In practice, only combinations of the tree conditional probabilities $p(T \mid Y)$ are actually computed. Kirshner (2008) further shows that all the P_{jk} 's can be computed at once with the same complexity $O(p^3)$, although the calculation may lead to numerical instabilities for large n and p.

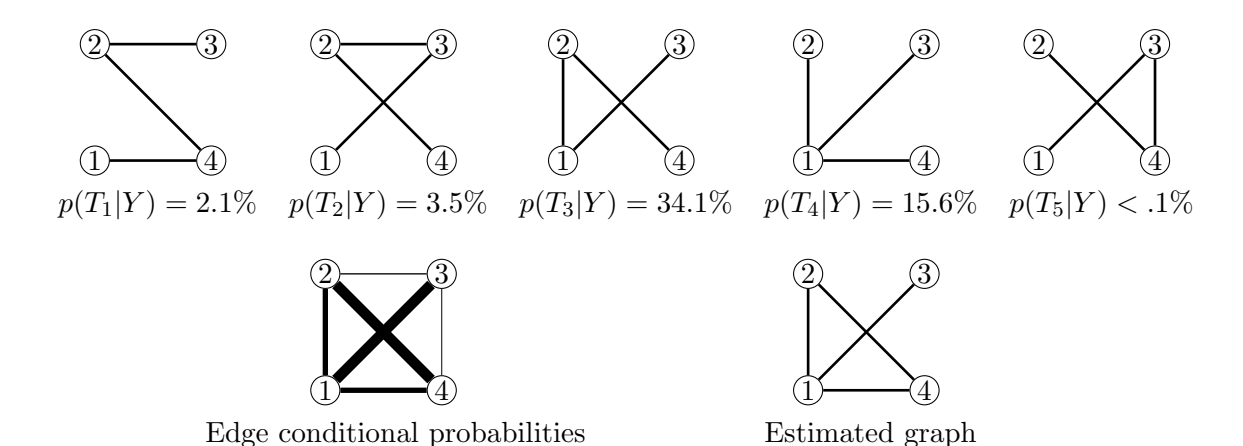


Figure 2: Tree averaging principle. Top: a subset of 5 spanning trees with 4 nodes, with their respective conditional probability given the data $p(T \mid Y)$. Bottom left: The weighted graph resulting from tree averaging. Each edge (j,k) has width proportional to its conditional probability. Bottom right: The estimated graph (obtained by thresholding edge probabilities) is not a tree.

M step: Estimating the β_{jk} . Maximizing (5) with respect to each of the β_{jk} is not straightforward, as the normalizing constant $B = \sum_{T} \prod_{(j,k) \in T} \beta_{jk}$ involves all β_{jk} 's. Still, the gradient of (5) can be computed using Lemma 2 from Meilă and Jaakkola (2006) (recalled as Lemma 1 in Appendix A.3), which also builds upon the Matrix Tree theorem (see Appendix A.2).

Algorithm output: edge scoring and network inference EMtree provides the (approximate) conditional probability P_{jk} for each edge (j,k) to be part of the network.

Hence, an estimate \widehat{G} of the network can be easily obtained by thresholding conditional probabilities: for a given threshold $0 < \lambda < 1$, the edge (j, k) will be in \widehat{G} if $P_{jk} \ge \lambda$. Fig. 2 (bottom right) illustrates that the resulting graph has no reason to be a tree. As our model is build on a tree hypothesis, a natural rule is to select the edges with probability P_{jk} greater than the probability for an edge to be part of a tree drawn uniformly, that is $\lambda = 2/p$.

To get a more robust estimate \widehat{G} , a resampling procedure can be designed in the spirit of the stability selection proposed by Liu et al. (2010). S sub-samples are drawn, each using a fraction f of available observations. For each sub-sample $s=1\ldots S$, an estimate \widehat{G}^s is made of the edges having probability $P_{jk}^s \geq 2/p$. Only edges selected in more than a fraction f' of the estimated graphs \widehat{G}^s are kept to build the final \widehat{G} . This procedure can be parallelized in an obvious manner. In all simulations and applications, we set f=80%. f' is a more flexible threshold; we set f'=80% in all simulations, and f'=90% in all applications.

2.3 Simulation and illustrations

The first part of the study relies on synthetic abundance datasets simulated according to a known network. We focus on three main factors which may affect the accuracy of EMtree: the dataset dimensions (number of samples/number of species), the structure of the network to be recovered (tree-shaped, uniform, clustered), and its density (expected proportion of connected pairs). The second part of the study is dedicated to the analysis of two ecological datasets using EMtree.

2.3.1 Alternative methods

Two methods based on transformed counts. SPIEC-EASI (Kurtz et al., 2015, R package SpiecEasi) and gCoda (Fang et al., 2017, code available on GitHub) both consist in transposing the inference problem in a continuous space by transforming count data into compositional data. SPIEC-EASI resorts to a centered log-ratio (clr) transformation of the counts directly, while gCoda takes advantage of the data compositionality and applies the log transformation to the relative counts. Both methods assume that the transformed counts have a joint Gaussian distribution, and that ecological networks are sparse. The network is then reconstructed using the graphical lasso (Friedman et al., 2008).

MInt (Biswas et al., 2016). The R package MInt is designed to learn microbial direct interactions, using the same Poisson mixed model as we do. However its inference method is quite different from ours as the Z_{ij} are first considered as random variables and then as fixed parameters. Like SPIEC-EASI and gCoda, MInt resorts to a glasso penalization to enforce network sparsity. The corresponding iterative algorithm bears a high computational cost dut to the large number of parameters to estimate.

Edge scoring and covariates. These three alternative methods build upon glasso penalization. For each edge score, there exists a minimal penalty value above which the edge is eliminated from the network. The higher this minimal penalty, the more reliable the edge in the network, so it can be used as a score reflecting the importance of an edge. Such score matrices can be built for SpiecEasi and gCoda, which provide the whole penalization paths, but not for MInt as it only gives access to the final estimated of the network.

SPIEC-EASI and gCoda cannot take covariates into account. In order to draw a fair comparison, we give these methods access to the covariate information by feeding them with residuals of the linear regression of the transformed data onto the covariates.

2.3.2 Comparison criteria

Each inference method performance is assessed by comparing the resulting network to the originally simulated graph. Quantities of truly present or absent edges are compared with quantities of detected or undetected edges.

FDR and density ratio criteria. Inferred networks are mostly useful to detect potential interactions between species, which then need to be tested to determine their exact nature. Falsely including an edge would lead to a loss of time and effort. Two main qualities are thus desirable for any network inference method: sparsity and few false discoveries. A network with a few reliable edges will be preferred to one having more edges with a larger risk of possible false discoveries. Therefore we choose the False Discovery Rate as evaluation criterion, which should be close to 0. Comparing FDR's only makes sense for networks with similar density. We then compute the ratio between the densities of the inferred and the true network (density ratio).

AUC criterion. The Area Under the Curve (AUC) criterion allows to evaluate the quality of the inferences without depending on a given thresholding method. The AUC gives the probability for a method to score the presence of a randomly selected present edge higher than that of a randomly selected absent one; it should be close to 1. Note that this criterion cannot be computed for MInt since this algorithm provides a unique solution without possibility of changing the minimal penalty value.

2.3.3 Simulation design

Simulated networks. We consider networks G with three typical structures: Scale-free, Erdös (short for Erdös-Reyni) and Cluster. Scale-free structure bears the closest similarity to the tree one, with almost the same density and no loops; it is popular in social networks and in genomics as it corresponds to a preferential-attachment behavior. It is simulated following the Barbási-Albert model as implemented in the huge R package (Zhao et al., 2012). The degree distribution of Scale-free structure follows a power law, which constrains the edges probabilities such that the network density cannot be controlled. The Erdös structure is the most even as the edges all have the same existence probability. It is a step away from the tree as it may contain loops; its density can be increased arbitrarily. The Cluster structure corresponds to a graph where the edges are spread into highly connected clusters, with few connection between the clusters. A Cluster graph can include many loops and therefore represents the most challenging structure for EMtree. We used the R package huge to generate all structures except for Clusters which we coded for better structure control through density and within/between cluster connection probability ratio (ratio parameter).

Simulation model. Data is simulated under the Poisson mixed model. We first build Σ_G following Zhao et al. (2012) and we simulate $\mathbf{Z}_i \sim \mathcal{N}(0, \Sigma_G)$. Then, we simulate count data Y according to (1) using a set of three covariates: one continuous variable, one ordinal and one categorical variable, both with five levels.

Simulation parameters. For each set of parameters and type of structure we generate 100 graphs, simulate a dataset and infer the dependency structure using EMtree, gCoda, SpiecEasi and MInt (for the first experiment).

To evaluate the influence of data dimension, we designed two scenarios: easy (n = 100, p = 20), and hard (n = 50, p = 30). Network density for Erdös and Cluster structures is set to $\log(p)/p$: it is higher in the hard than in the easy case, and higher than tree structures.

As for the effect of structures, wide ranges of values for each parameter provide a general idea of the behaviour of methods. For comparison's sake, the same density is fixed for all structures in this case, so that only n and p vary in turn; the scale-free structure imposes a common density of 2/p. Default values for n and p are respectively 100 and 20.

Finally, this simulation study assess the robustness of EMtree to the tree assumption. AUC measures are collected for variations of n and p with a density of 5/p, as well as for variations of parameters controlling the network density.

All computation times have been obtained with a 2.5 GH Intel Core 17 processor and 8 G of RAM.

2.3.4 Illustrations

The first application deals with fish population measurements in the estuary of the Fatala River, Guinea, (Baran, 1995, available in the R package ade4). The data consists of 95 count samples of 33 fish species, and available covariates are the date and site. We inferred the network using four models including no covariates, either one or both covariates (i.e. respectively the null, site, date and site+date models)

The second example is a metabarcoding experiment designed to study oak powdery mildew (Jakuschkin et al., 2016), caused by the fungal *Erysiphe alphitoides* (Ea). To study the pathobiome of oak leaves, measurements were done on three trees with different infection status. The resulting dataset is composed of 116 count samples of 114 fungal and bacterial operational taxonomic units (OTUs) of oak leaves, including the Ea agent. Several covariates are available,

among which the tree status, and three covariates we call D1 to D3 measuring the distances of oak leaves to the ground, to the base of the branch, and to the tree trunk. Metabarcoding experiments set different depths of coverage for each OTU, which must be accounted for. We fitted three Poisson mixed models including these depths as offsets, and either none, the tree status or all of the covariates (i.e. respectively null, tree, and tree+D1+D2+D3 models).

To further analyse the inferred networks, we use the betweenness centrality (Freeman, 1978), a centrality measure used particularly in social network analysis. It measures how many shortest paths pass through a given node; it can be seen as a measure of a node's ability to act as a bridge. High betweenness measures therefore identify key nodes that are sensitive points and can efficiently describe a network structure. We use the R package *igraph* to compute these measures.

3 Results

3.1 On simulated data

3.1.1 Effect of dataset dimensions

We study how the different approaches behave on an easy setting (n = 100, p = 20) and a hard setting (n = 50, p = 30). Fig. 3 displays FDR and log of density ratio measures for all methods on the different cases. A first general result is that, even when the network density is well estimated, all methods yield FDR of 10%-30%, even in the easy case. This reminds that network inference from abundance data is a difficult task, and that perfect reconstruction of the network remains an out-of-reach goal.

When comparing the different approaches, gCoda and SpiecEasi turn out to provide very sparse networks. In the easy setting they returned an empty graph for 19% and 23% of the simulations respectively, and 46% and 25% in the hard setting. This could be due to their optimization process which is complex to configure. The extreme FDR scores of gCoda and SpiecEasi result from their low number of detected edges. When moving from the easy to the hard cases, SpiecEasi density ratio remains more or less the same and its FDR worsen. In contrast, both the density ratio and the FDR of gCoda decrease, meaning that it detects reliable but fewer edges. The MInt method displays the opposite behavior with very high density ratios (sometimes two to three times more edges as in the original network) and high FDRs; both measures increase when moving from easy to hard problems.

EMtree shows density ratios close to 1 for all structures, whatever the difficulty level. Its FDR medians are between those of gCoda and MInt, and increase in hard settings. As a consequence, the proposed methodology compares well to existing tools on problems with varying difficulties. As for running times gathered in Table 1, EMtree is between SpiecEasi and MInt in both easy and hard cases. For the sake of comparison with SpiecEasi these times correspond to the same S=150. However Fig. 4 shows EMtree FDR and density ratio measures for S between 1 and 150. Clearly, the performances stabilize from about S=10. Therefore the same results can be reached with much lower S values. For example S=20 seems a reasonable choice of settings here, and running times would then be lower than those of MInt in all cases according to Table 2.

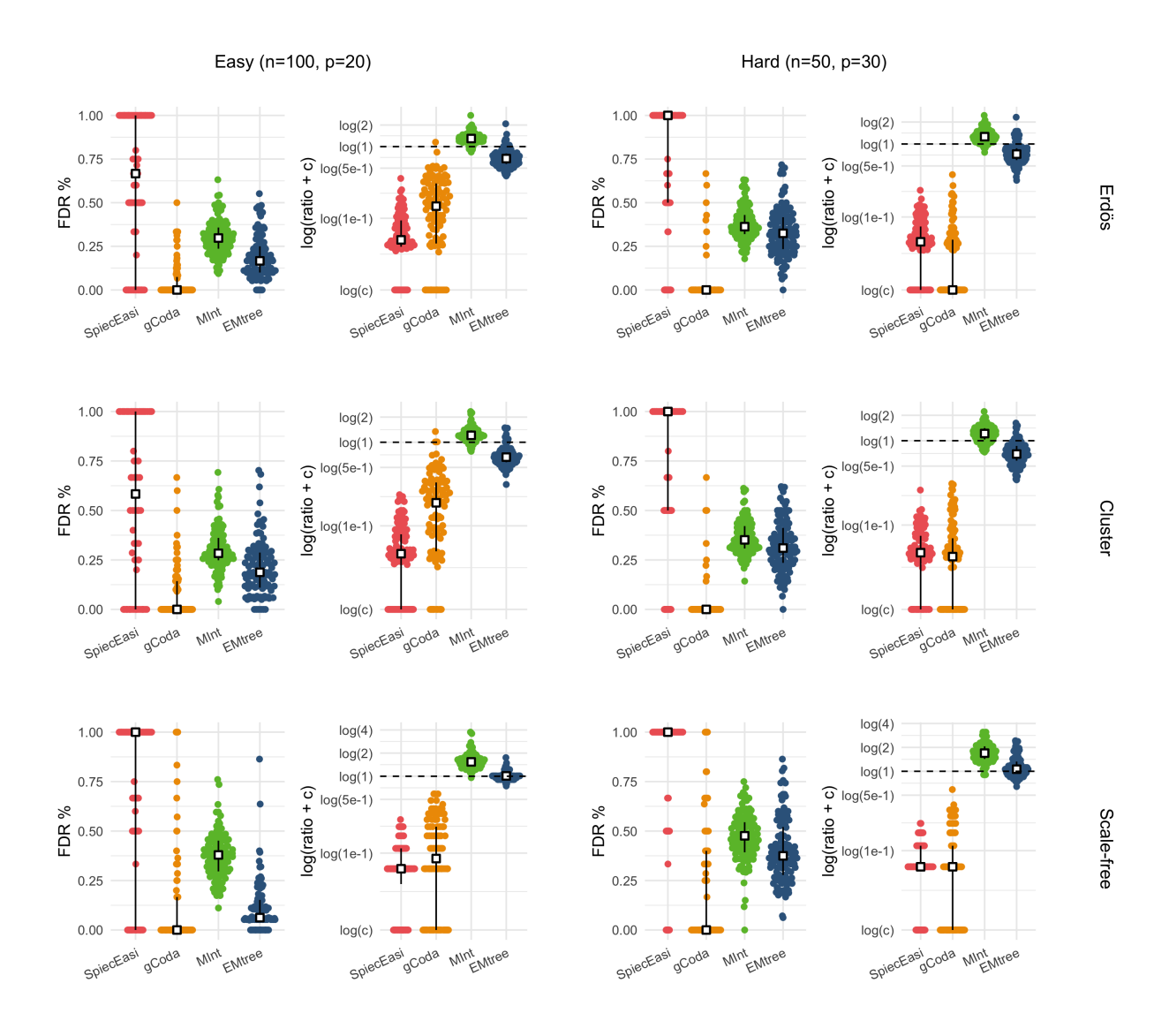


Figure 3: FDR and log density ratio measures for all methods at two different difficulty levels and 100 networks of each type. White squares and black plain lines represent medians and quartiles respectively. c = 0.01. S = 150 for SpiecEasi and EMtree. SpiecEasi and gCoda lambda grid parameters: lambda.min.ratio = 0.01 and nlambda = 30.

	gCoda	MInt	EMtree	SpiecEasi
Easy	0.05 (0.02)	27.89(9.2)	91.47 (9.41)	112.54 (5.23)
Hard	0.05 (0.02)	40.48 (18.27)	68.91 (9.19)	112.7(4.94)

Table 1: Median and standard-deviation running-time values (in seconds), including resampling with S=150 for SpiecEasi and EMtree.

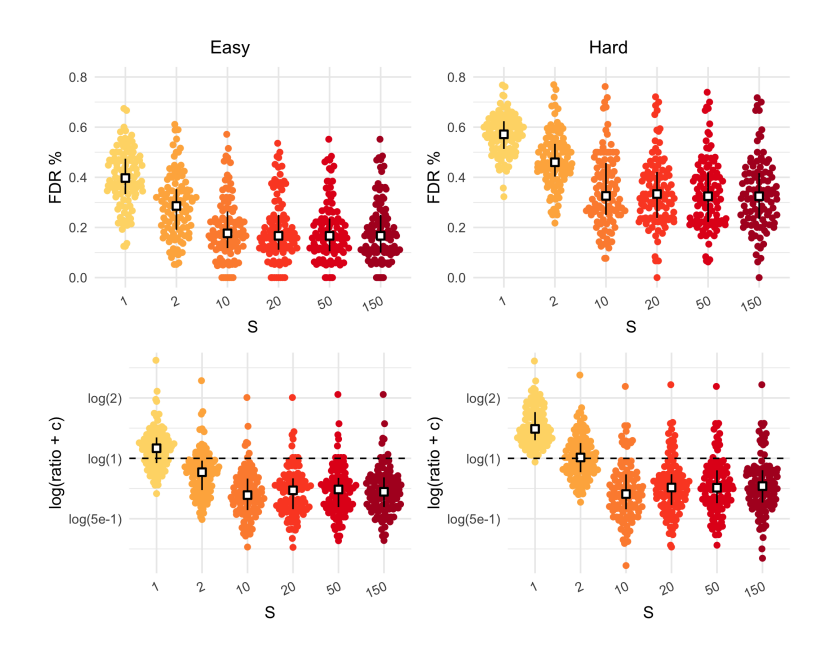


Figure 4: FDR and density ratio measures of EMtree with varying values of S (Erdös structure).

\mathbf{S}	1	2	10	20	50	150
Easy	0.66(0.15)	1.86(0.23)	7(0.81)	12.29(1.27)	29.5(3.39)	87.3(10.36)
Hard	0.45(0.12)	1.44(0.14)	5.06(0.78)	8.97(0.87)	23.35(2.40)	69.29(10.83)

Table 2: Median and standard-deviation running-time values in seconds for inference of Erdös structure with EMtree and different values of S.

3.1.2 Effect of network structure

100 AUC values are obtained for each set of parameters and method. The results are summarized as medians and inter-quartile intervals in Fig. 5 (Scale-free structures) and in Fig. 6 (top) (Erdös and Cluster structures) .

As expected, the higher the number of observations, the better the performance, for all methods and structures. Increasing the number of species, on the other hand, appears to impair the performance of SpiecEasi in all cases, and of EMtree in Scale-free structures only. gCoda outperforms SpiecEasi for Erdös and Clusters structures, except for small values of p (p < 15). As EMtree had almost always perfect scores for Scale-free networks with n = 100, we lowered this parameter to 30. On the right of Fig. 5 we see performance deteriorating along with p for all methods, including for EMtree. However its AUC measures remains above 70% in median in the extreme case where p = n.

EMtree shows better performance the closer the structure is to that of a tree. Nevertheless, this method overall performs better than gCoda and SpiecEasi on all the structures studied. Running times are summarized in Table 3. EMtree is about 10 times slower than gCoda (4 times for small n), and 4 times faster than SpiecEasi. The high standard deviation for small n seems to be due to gCoda struggling with Scale-free structures.

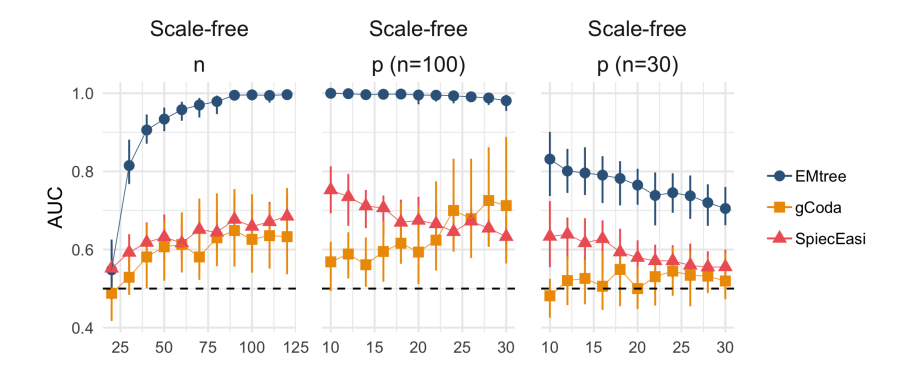


Figure 5: Effect of Scale-free structure on AUC medians and inter-quartile intervals for parameters n and p.

	n < 50	$n \ge 50$	p < 20	$p \ge 20$
EMtree	0.44 (0.14)	0.6 (0.17)	0.41 (0.13)	0.76 (0.21)
gCoda	0.11 (26.8)	0.05 (0.05)	0.05 (0.04)	0.09(0.54)
SpiecEasi	2.09 (0.26)	2.37(0.28)	2.42(0.27)	2.42(0.26)

Table 3: Median and standard-deviation of running times for each method in seconds, for n and p parameters.

3.1.3 Effect of network density

Similarly to the previous experiment, 100 AUC values per set of features are recorded. Fig. 7 summarizes the measures for a varying graph density, with fixed parameters n and p. It shows in details the performance degradation for all methods along with the network density. gCoda performance deteriorates faster than that of the other methods: its outcomes are close to EMtree's for a 2/p density, and below SpiecEasi's for a 5/p density. Fig. 6 (bottom) presents AUC measures for variations of n and p parameters with a fixed density of 5/p. Overall EMtree compares well to the two other methods, except for very small values of p where SpiecEasi shows a better performance. Finally, the graph density does not seem to impact running times for parameters n and p (not shown).

Despite EMtree good performance, the main conclusion is that network reconstruction gets harder as the network gets denser.

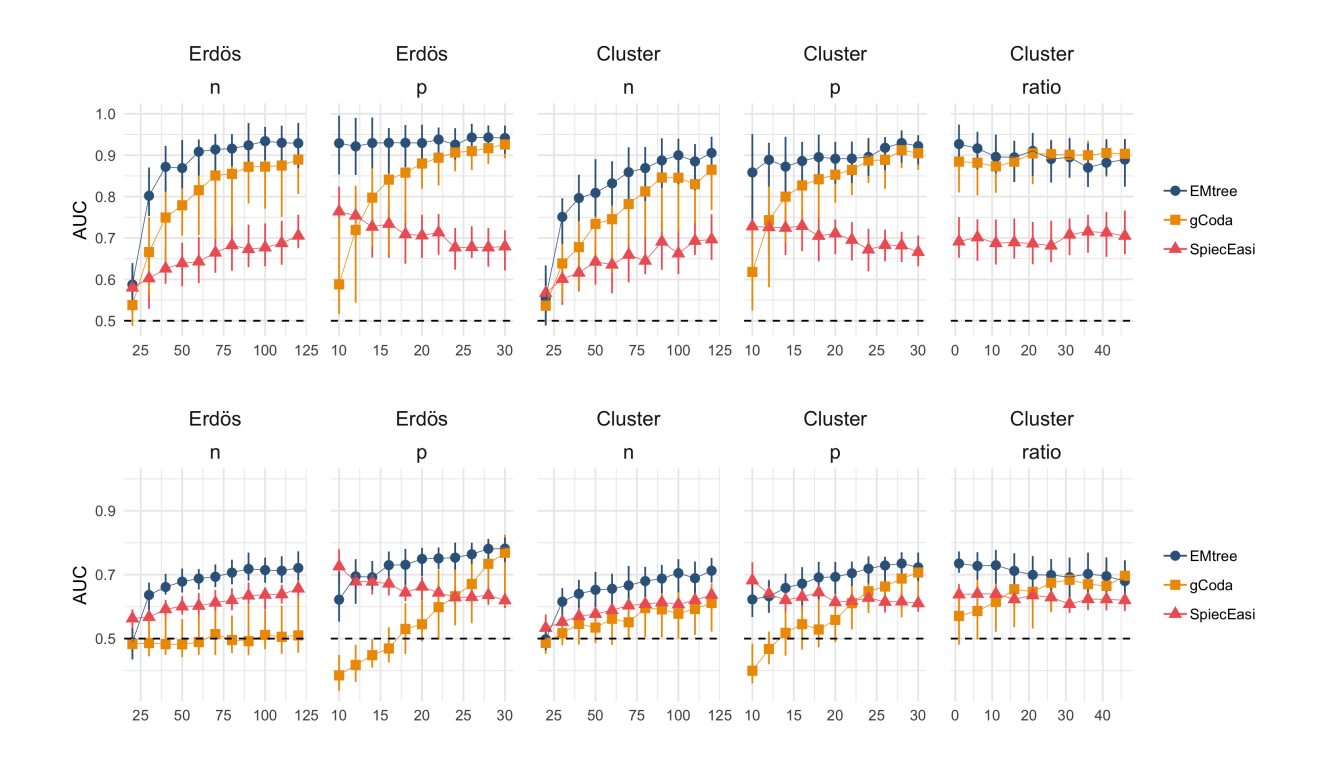


Figure 6: Effect of Erdös and Cluster structures on AUC medians and inter-quartile intervals for parameters n, p and ratio. Top: densities set to 2/p, bottom: densities set to 5/p.

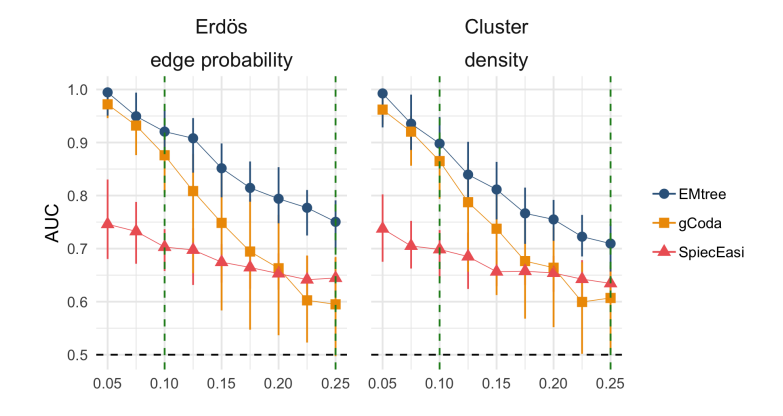


Figure 7: AUC median and inter-quartile intervals for parameters controlling the number of edges in Erdös (edge probability) and in Cluster (density) structures. Two vertical dashed lines identify the 2/p and 5/p densities. p = 20, n = 100

3.2 Illustrations

Most frequently, introducing a covariate results in reducing the number of edges (i.e. sparser networks). However new edges can appear as well, as adjusting for a covariate also reduces the variability, which improves the detection power. In our approach the number of edges also depends on the selection threshold f', as shown by Fig. 9. The curves on this figure are very smooth, illustrating the difficulty of setting this threshold.

3.2.1 Fish populations in the Fatala River estuary

The networks shown in Fig. 8 were obtained with S=100 sub-samples, each of which took about 0.3s to be inferred with EMtree. On each network, the three species with the highest betweenness scores are highlighted; the corresponding species names are given in Appendix B.2.1. These networks suggest a predominant role of the *site* covariate compared to the *date*. Indeed, adjusting for the *site* results in much sparser networks. Besides it deeply modifies the network structure: the *site* network has more new edges (12) than it has edges in common (6) with the *null* network. In addition, the nodes highlighted on the network *site* are completely different from those of the network *null*, and yet remain the same when introducing the *date* covariate. This suggests that the environmental heterogeneity between the sites has a major effect on the species distribution, while the effect of the date of sampling is moderate.

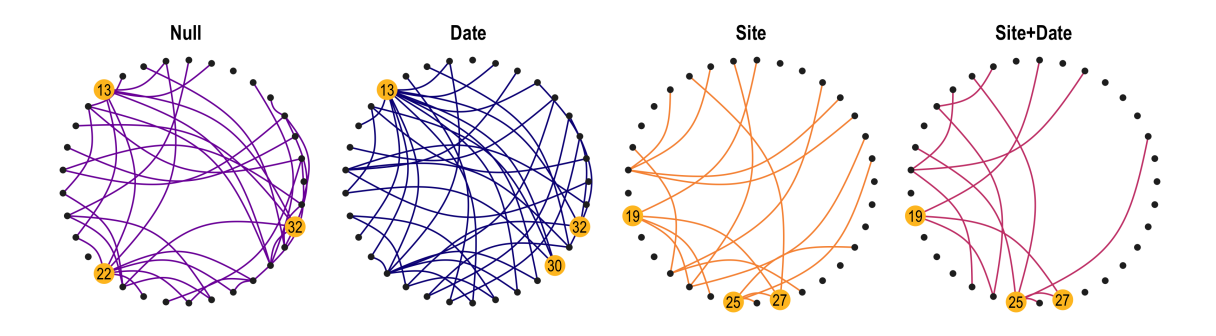


Figure 8: Interaction networks of Fatala River fishes inferred when adjusting for none, both or either one of the covariates among *site* and *date*. The nodes highlighted correspond to the three highest betweenness centrality scores. S = 100, f' = 90%.

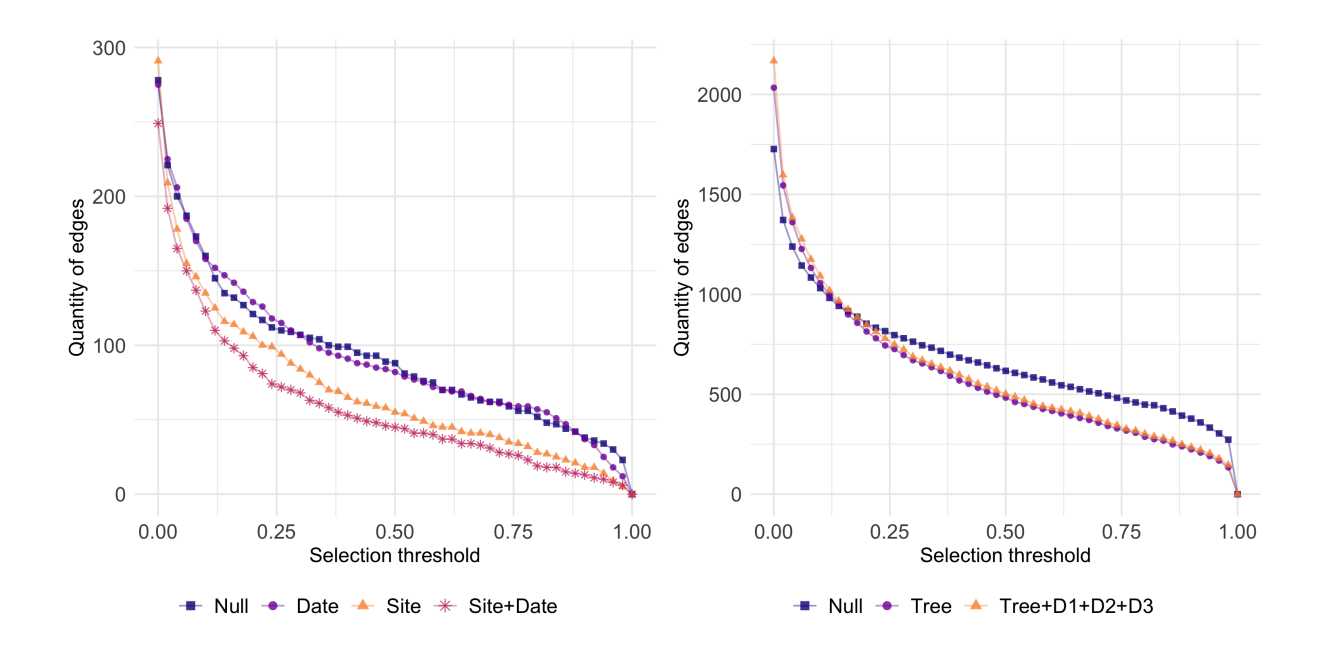


Figure 9: Quantity of selected edges as a function of the selection threshold (*left*: Fatala fishes, *right*: oak mildew.)

3.2.2 Oak powdery mildew

The networks presented on Fig. 10 were obtained using S = 100 sub-samples as well. Running EMtree on each of them took about 14s. Each network highlights the six nodes with the highest betweenness scores and the connections of Ea.

When providing the inference with more information (tree status, distances), the structure of the resulting network is significantly modified. This can be pointed out when looking at variations in the betweenness scores (the highlighted nodes differ from one model to another), as well as changes in the networks density. Fig. 9 (right) shows an important gap in density between the null model and the others, starting from a 25% selection threshold. From a more biological point of view, the features of the Ea node are greatly modified too: its betweenness score is among the smallest in the null network (quantile 17%), and among the highest in the two other networks (quantiles 93% and 78%). Obviously, its connections to the other nodes undergo changes as well. So here taking covariates into account results in less interactions with the pathogen, and a greater role of the latter in the pathobiome organization.

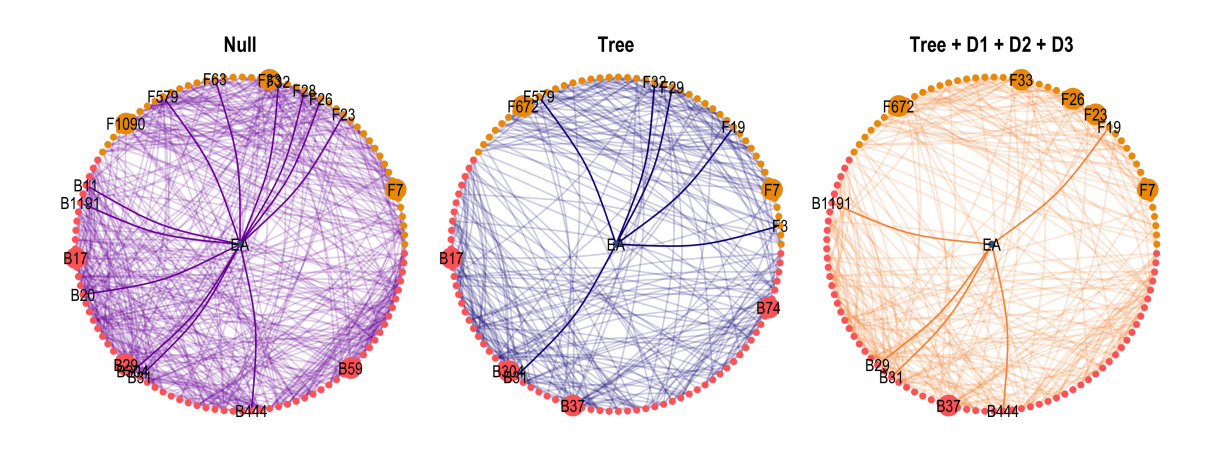


Figure 10: Ea interaction networks on oak leaves inferred with EMtree when adjusting for none, the *tree* covariate or all covariates. Bigger nodes represent OTUs with highest betweenness values, colours differentiate fungal and bacterial OTUs. S = 100, f' = 90%.

Following a Bayesian approach, Jakuschkin et al. (2016) identifies a list of 26 OTUs likely to be directly interacting with Ea, as well as a list of 34 OTUs significantly associated with infected samples. We compare this list of 52 OTUs to EMtree results when varying the selection threshold f'. On Fig. 11 the fraction of OTUs identified by EMtree and shared with the previous study seems to stabilize around 70%, showing these outcomes reasonable consistency. Note that for EMtree to identify about the same quantity of OTUs as Jakuschkin et al. (2016), the selection threshold must be set between 10% and 15%, which seems low to us.

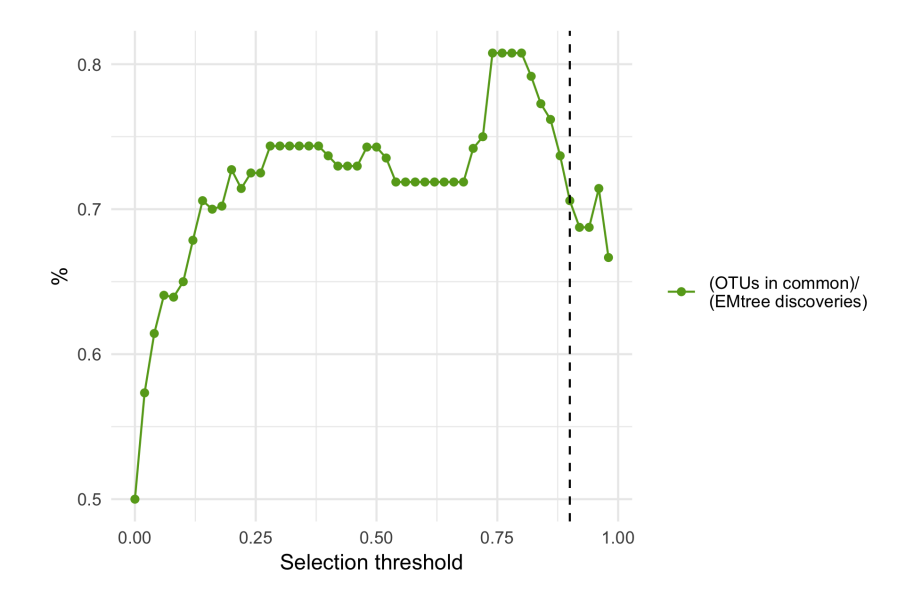


Figure 11: Proportions among EMtree results of OTUs common to both approaches.

For a sufficiently high threshold, it would be interesting to have a closer look at the disagreements between the two studies. Table 5 in Appendix B details the outcomes comparison obtained with a 90% threshold for EMtree. This shows our approach finds four potential neighbors of Ea which were not identified by Jakuschkin et al. (2016), among which three (F29, F32 and F579) are neighbors in the *tree* model but not in the last model. This suggests that these connections are involved in the spatial spread of the pathogen in the oak tree. However, further investigations would be required to better understand the role of these unidentified OTUs.

4 Discussion

The reconstruction of ecological networks is a challenging task, for which a series of methods have been proposed in the past years. Abundance data seems to be a promising source of information for this purpose. Here we adopt the formalism of graphical models to define a probabilistic model-based framework for the inference of ecological networks from abundance data. Using a model-based approach offers several important advantages. First, it enables us to easily and explicitly account for environmental and experimental effects. Then, as it also relies on a formal statistical definition of an ecological network in the context of graphical models, accounting for abiotic effects and modelling species interactions are two clearly defined and distinguished goals. Finally, all the underlying assumptions are explicitly stated in the model definition itself, and can therefore be discussed and criticized.

We developed an efficient method to infer sparse ecological networks, which combines a multivariate Poisson mixed model for the joint distribution of the species abundances, with an averaging over all spanning trees to efficiently infer direct species interactions. As we do consider a mixture over all spanning trees, the model does not assume that the underlying network is tree-like: it remains flexible for modeling most types of statistical dependencies. An EM algorithm maximizes the likelihood of the result and gives probabilities for each edge to be part of the network as an output. The final interaction network is obtained after a resampling step to increase its robustness.

The proposed EMtree methodology performs very well when compared with state-of-the-art approaches. In particular, it provides sparser network than MInt with lower false discovery rate,

and it better identifies interactions in presence of covariates than gCoda and SpiecEasi. Two illustrations show the dramatic effect of covariates on the structure of the inferred network. Experiments on simulated data and illustrations also demonstrate that EMtree computational cost remains very reasonable.

The proposed methodology could be extended in several ways. The effect of the covariates could be modelled in a more flexible way using generalized additive models, which include non-linear effects (Hastie, 2017). Besides, ecological abundance data is usually collected in spatially organized sites. Taking spatial autocorrelation would obviously improve the relevance of the proposed model. Since our model implies a latent structure, a natural way to take spatial dependencies into account would be to introduce a correlation between the latent vectors associated with each site, as done in multivariate geostatistical processes (Cressie, 1992). It is also very likely that not all covariates nor even all species have been measured or observed. Another extension may therefore be to detect ignored covariates or missing species. To this purpose EMtree could probably be combined with the approach developed by Robin et al. (2018) to identify missing actors. Lastly, networks comparison is a wide and interesting question and tools lack to check which edges are shared by a set of networks. Here, the approach introduced by Schwaller and Robin (2017) could be adapted to the EMtree framework.

Data accessibility. The method developed in this paper is implemented in the R package EMtree available on GitHub: https://github.com/Rmomal/EMtree.

Acknowledgement. The authors thank P. Gloaguen and M. Authier for helpful discussions and C. Vacher for providing the oak data set. This work is partly funded by ANR-17-CE32-0011 NGB and by a public grant as part of the Investissement d'avenir project, reference ANR-11-LABX-0056-LMH, LabEx LMH.

Author's contributions statement. All authors conceived the ideas and designed methodology; R. Momal developed and tested the algorithm. All authors led the writing of the manuscript, contributed critically to the drafts and gave final approval for publication.

References

- J. Aitchison and C.H Ho. The multivariate Poisson-log normal distribution. *Biometrika*, 76(4): 643–653, 1989.
- M. Austin. Species distribution models and ecological theory: a critical assessment and some possible new approaches. *Ecological modelling*, 200(1-2):1–19, 2007.
- E. Baran. Dynamique spatio-temporelle des peuplements de Poissons estuariens en Guinée (Afrique de l'Ouest). PhD thesis, Thèse de Doctorat, Université de Bretagne Occidentale, 1995.
- S. Biswas, M. McDonald, D. S Lundberg, J. L. Dangl, and V. Jojic. Learning microbial interaction networks from metagenomic count data. *Journal of Computational Biology*, 23(6): 526–535, 2016.
- S. Chaiken and D. J. Kleitman. Matrix tree theorems. *Journal of combinatorial theory, Series* A, 24(3):377–381, 1978.
- J. Chiquet, M. Mariadassou, and S. Robin. Variational inference for probabilistic Poisson PCA. Technical report, arXiv:1703.06633, 2017. to appear in *Annals of Applied Statistics*.

- C. Chow and C. Liu. Approximating discrete probability distributions with dependence trees. *IEEE Transactions on Information Theory*, 14(3):462–467, May 1968.
- N. Cressie. Statistics for spatial data. Terra Nova, 4(5):613–617, 1992.
- A. P. Dempster, N. M. Laird, and D. B. Rubin. Maximum likelihood from incomplete data via the EM algorithm. *J. Royal Statist. Soc.*, series B, 39:1–38, 1977.
- J. Elith and J. R. Leathwick. Species distribution models: ecological explanation and prediction across space and time. *Annual review of ecology, evolution, and systematics*, 40, 2009.
- D. M Evans, J. JN Kitson, D. H Lunt, N. A Straw, and M. JO Pocock. Merging dna metabarcoding and ecological network analysis to understand and build resilient terrestrial ecosystems. *Functional ecology*, 30(12):1904–1916, 2016.
- H. Fang, C. Huang, H. Zhao, and M. Deng. gCoda: conditional dependence network inference for compositional data. *Journal of Computational Biology*, 24(7):699–708, 2017.
- K. Faust and J. Raes. Microbial interactions: from networks to models. *Nature Reviews Microbiology*, 10(8):538, 2012.
- L. C Freeman. Centrality in social networks conceptual clarification. *Social networks*, 1(3): 215–239, 1978.
- J. Friedman, T. Hastie, and R. Tibshirani. Sparse inverse covariance estimation with the graphical lasso. *Biostatistics*, 9(3):432–441, 2008.
- T. J Hastie. Generalized additive models. In *Statistical models in S*, pages 249–307. Routledge, 2017.
- B. Jakuschkin, V. Fievet, L. Schwaller, T. Fort, C. Robin, and C. Vacher. Deciphering the pathobiome: Intra- and interkingdom interactions involving the pathogen erysiphe alphitoides. *Microb Ecol*, 72(4):870–880, 2016.
- P. Jordano. Sampling networks of ecological interactions. Functional Ecology, 30(12):1883–1893, 2016.
- S. Kirshner. Learning with tree-averaged densities and distributions. In *Advances in Neural Information Processing Systems*, pages 761–768, 2008.
- Z. D. Kurtz, C. L. Müller, E. R. Miraldi, D. R. Littman, M. J. Blaser, and R. A. Bonneau. Sparse and compositionally robust inference of microbial ecological networks. *PLoS computational biology*, 11(5):e1004226, 2015.
- S. L. Lauritzen. Graphical Models. Oxford Statistical Science Series. Clarendon Press, 1996.
- H. Liu, K. Roeder, and L. Wasserman. Stability approach to regularization selection (stars) for high dimensional graphical models. In *Proceedings of the 23rd International Conference on Neural Information Processing Systems - Volume 2*, NIPS'10, pages 1432–1440, USA, 2010. Curran Associates Inc. URL http://dl.acm.org/citation.cfm?id=2997046.2997056.
- M. Meilă and T. Jaakkola. Tractable bayesian learning of tree belief networks. *Statistics and Computing*, 16(1):77–92, 2006.
- N. Morueta-Holme, B. Blonder, B. Sandel, B. J. McGill, R. K. Peet, J. E. Ott, C. Violle, B. J. Enquist, P. M. Jørgensen, and J-C. Svenning. A network approach for inferring species associations from co-occurrence data. *Ecography*, 39(12):1139–1150, 2016.

- T. Poisot, D. B Stouffer, and S. Kéfi. Describe, understand and predict: why do we need networks in ecology? *Functional Ecology*, 30(12):1878–1882, 2016.
- S. A Richards. Dealing with overdispersed count data in applied ecology. *Journal of Applied Ecology*, 45(1):218–227, 2008.
- G. Robin, C. Ambroise, and S. Robin. Incomplete graphical model inference via latent tree aggregation. *Statistical Modelling*, page 1471082X18786289, 2018.
- L. Schwaller and S. Robin. Exact bayesian inference for off-line change-point detection in tree-structured graphical models. *Statistics and Computing*, 27(5):1331–1345, 2017.
- L. Schwaller, S. Robin, and M. Stumpf. Bayesian Inference of Graphical Model Structures Using Trees. Technical Report 1504.02723, arXiv, April 2015.
- W. Ulrich and N. J. Gotelli. Null model analysis of species associations using abundance data. Ecology, 91(11):3384-3397, 2010.
- A. Valiente-Banuet, M. A Aizen, J. M. Alcántara, J. Arroyo, A. Cocucci, M. Galetti, M. B García, D. García, J. M Gómez, P. Jordano, et al. Beyond species loss: the extinction of ecological interactions in a changing world. *Functional Ecology*, 29(3):299–307, 2015.
- D. I. Warton, F. G. Blanchet, R. B. O'Hara, O. Ovaskainen, S. Taskinen, S. C Walker, and F. KC. Hui. So many variables: joint modeling in community ecology. *Trends in Ecology & Evolution*, 30(12):766–779, 2015.
- T. Zhao, H. Liu, K. Roeder, J. Lafferty, and L. Wasserman. The huge package for high-dimensional undirected graph estimation in R. Journal of Machine Learning Research, 13 (Apr):1059–1062, 2012.

A Supplement: Methods

A.1 Variational EM in the observed layer

To estimate the fixed regression parameters gathered in $\boldsymbol{\theta}$, we resort to a surrogate model where the entries of the abundance matrix \mathbf{Y} still have the conditional distribution given in (1), but where the distribution of the \mathbf{Z}_i is not constrained to be faithful to a specific graphical model. Namely, the latent vectors \mathbf{Z}_i are only supposed to be independent and identically distributed (iid) Gaussian with distribution $\mathcal{N}(0, \mathbf{\Sigma})$, without any restriction on $\mathbf{\Sigma}$.

This surrogate model is actually a Poisson log-normal model as introduced by Aitchison and Ho (1989), the parameters of which can be estimated using a variational approximation similar to this introduced in Chiquet et al. (2017). Namely, instead of maximizing the log-likelihood $\log \mathbb{P}\{Y\}$ with respect to the parameters $\boldsymbol{\theta}$ and $\boldsymbol{\Sigma}$ using a regular EM algorithm, we maximize the lower bound of it

$$\mathcal{J}(Y; \boldsymbol{\theta}, \boldsymbol{\Sigma}, \widetilde{P}) := \log P_{\boldsymbol{\beta}, \boldsymbol{\Sigma}}(Y) - KL\left(\widetilde{P}(Z) || P_{\boldsymbol{\beta}, \boldsymbol{\Sigma}}(Z \mid Y)\right),$$

where KL(P||Q) stands for Küllback-Leibler divergence between distribution P and Q and where the distribution $\widetilde{P}(\mathbf{Z})$ (which approximates $\widetilde{P}_{\beta,\Sigma}(Z\mid Y)$) is chosen to be Gaussian. This means that each conditional distribution $P(\mathbf{Z}_i\mid \mathbf{Y}_i)$ is approximated with a normal distribution $\mathcal{N}(\widetilde{m}_i,\widetilde{S}_i)$. As shown in Chiquet et al. (2017), $\mathcal{J}(Y,\boldsymbol{\theta},\Sigma,\widetilde{P})$ is bi-concave in (Θ,Σ) and $\{(\widetilde{m}_i,\widetilde{S}_i)_i\}$, so that gradient ascent can be used. The PLNmodels R-package –available on GitHub– provides an efficient implementation of it.

The entries of the \widetilde{m}_i and S_i provide us with approximations of the conditional expectation, variance and covariance of the Z_{ij} conditionally on the \mathbf{Y} , which we use to get the estimates $\widehat{\sigma}_j^2$ and $\widehat{\rho}_{jk}$ given in (7). More specifically, we use $\mathbb{E}(Z_{ij} \mid \mathbf{Y}_i) \simeq \widetilde{m}_{ij}$, $\mathbb{E}(Z_{ij}^2 \mid \mathbf{Y}_i) \simeq \widetilde{m}_{ij}^2 + \widetilde{S}_{i,jj}$ and $\mathbb{E}(Z_{ij}Z_{ik} \mid \mathbf{Y}_i) \simeq \widetilde{m}_{ij}\widetilde{m}_{ik} + \widetilde{S}_{i,jk}$.

A.2 EM in the latent layer

Complete log-likelihood conditional expectation

Because of the specific form given in (3), and because the $\mathbf{Z}_i \mid T$ are Gaussian, we have that

$$\log p_{\Sigma}(Z|T) = \sum_{j=1}^{p} \sum_{i=1}^{n} \log P(Z_{ij}|T) + \sum_{(j,k)\in T} \sum_{i=1}^{n} \log \left(\frac{P(Z_{ij}, Z_{ik})}{P(Z_{ij})P(Z_{ik})}\right)$$

$$= -\frac{n}{2} \log \sigma_{j}^{2} - \frac{1}{2} \sum_{j=1}^{p} \sum_{i=1}^{n} \frac{Z_{ij}^{2}}{\sigma_{j}^{2}} - \frac{n}{2} \sum_{(j,k)\in T} \log(1 - \rho_{jk}^{2})$$

$$-\frac{1}{2} \sum_{(j,k)\in T} \frac{1}{1 - \rho_{jk}^{2}} \sum_{i=1}^{n} \left(\rho_{jk}^{2} \frac{Z_{ij}^{2}}{\sigma_{j}^{2}} + \rho_{jk}^{2} \frac{Z_{ik}^{2}}{\sigma_{k}^{2}} - 2\rho_{jk} \frac{Z_{ij}Z_{ik}}{\sigma_{j}\sigma_{k}}\right) + \text{cst}$$
(6)

where the constant term does not depend on any unknown parameter. In the EM algorithm, we have to maximize the conditional expectation of (6) with respect to the variances σ_j^2 and the correlation coefficients ρ_{jk} . The resulting estimates take the usual forms, but with the conditional moments of the Z_{ij} , that is

$$\widehat{\sigma}_{j}^{2} = \frac{1}{n} \sum_{i} \mathbb{E}(Z_{ij}^{2} \mid \mathbf{Y}), \qquad \widehat{\rho}_{jk} = \frac{1}{n} \sum_{i} \mathbb{E}(Z_{ij} Z_{ik} \mid \mathbf{Y}) / (\widehat{\sigma}_{j} \widehat{\sigma}_{k}) . \tag{7}$$

which do not depend on T.

and the maximized conditional expectation of (6) becomes

$$\mathbb{E}\left(\log p_{\widehat{\Sigma}}(Z|T) \mid \mathbf{Y}\right) = -\frac{n}{2}\log\widehat{\sigma}_j^2 - \frac{n}{2}\sum_{(j,k)\in T}\log(1-\widehat{\rho}_{jk}^2) + \text{cst.}$$
(8)

We are left with the writing of the conditional expectation of the first two terms of the logarithm of (4), once optimized in Σ . Combining (2) and (8), and noticing that the probability for an edge to be part of the graph is the sum of the probability of all the trees than contain this edge, we get (denoting $\log \widehat{\psi}_{jk} = (1 - \widehat{\rho}_{jk}^2)^{-n/2}$)

$$\mathbb{E}\left(\log p_{\beta}(T) + \log p_{\widehat{\Sigma}}(Z \mid T) \mid Y\right) = \sum_{T \in \mathcal{T}} p(T \mid Y) \left(\log p_{\beta}(T) + \log p_{\widehat{\Sigma}}(Z \mid T)\right)$$

$$= -\log B + \sum_{T \in \mathcal{T}} p(T \mid Y) \sum_{(j,k) \in T} \left(\log \beta_{jk} + \log \widehat{\psi}_{jk}\right) + \operatorname{cst}$$

$$= -\log B + \sum_{(j,k)} \mathbb{P}\{(j,k) \in T \mid Y\} \left(\log \beta_{jk} + \log \widehat{\psi}_{jk}\right) + \operatorname{cst},$$

which gives (5).

As explained in the section above, we approximate expectations and probabilities conditional on Y by their variational approximation.

This provides us with the approximate conditional distribution of the tree T given the data Y:

$$\widetilde{p}(T|Y) = \prod_{jk \in T} \beta_{jk} \widehat{\psi}_{jk} / C,$$

where C is the normalizing constant: $C = \sum_{T} \prod_{j,k \in T} \beta_{jk} \widehat{\psi}_{jk}$. The intuition behind this approximation is the following: according to Eq. (2), the marginal probability a tree T is proportional to the product of the weights β_{jk} of its edges. The conditional distribution probability of tree is proportional to the same product, the weights β_{jk} being updated as $\beta_{jk}\widehat{\psi}_{jk}$, where $\widehat{\psi}_{jk}$ summarizes the information brought by the data about the edge (j,k).

Steps E and M

E step: From the above computation we get the following approximation:

$$\mathbb{P}(\{j,k\} \in T|Y) \simeq 1 - \sum_{T:jk \notin T} \widetilde{p}(T|Y),$$

and so we define p_{jk} as follows:

$$P_{jk} = 1 - \frac{\sum_{T:jk \notin T} \prod_{j,k \in T} \beta_{jk} \psi_{jk}}{\sum_{T} \prod_{j,k \in T} \beta_{jk} \psi_{jk}}.$$

 P_{jk} can be computed with Theorem 1, letting $[\mathbf{W}^h]_{jk} = \beta^h_{jk} \widehat{\psi}_{jk}$ and $\mathbf{W}^h_{\backslash jk} = \mathbf{W}^h$ except for the entries (j,k) and (k,j) which are set to 0. The modification of $\mathbf{W}^h_{\backslash jk}$ with respect to \mathbf{W}^h amounts to set to zero the weight product, and so the probability, for any tree T containing the edge (j,k). As a consequence, we get

$$P_{jk}^{h+1} = 1 - \left| Q_{uv}^*(\mathbf{W}_{\backslash jk}^h) \right| / \left| Q_{uv}^*(\mathbf{W}^h) \right|.$$

M step: Applying Lemma 1 to the weight matrix β , the derivative of B with respect to β_{ik} is

$$\partial_{\beta_{ik}}B = [\mathbf{M}(\boldsymbol{\beta})]_{jk} \times B$$

then the derivative of (5) with respect to β_{jk} is null for $\beta_{jk}^{h+1} = P_{jk}^{h+1} / [\mathbf{M}(\boldsymbol{\beta}^h)]_{jk}$.

A.3 Matrix tree theorem

For any matrix **W**, we denote its entry in row u and column v by $[\mathbf{W}]_{uv}$. We define the Laplacian matrix **Q** of a symmetric matrix $\mathbf{W} = [w_{jk}]_{1 \leq j,k \leq p}$ as follows:

$$[\mathbf{Q}]_{jk} = \begin{cases} -w_{jk} & 1 \le j < k \le p \\ \sum_{u=1}^{p} w_{ju} & 1 \le j = k \le p. \end{cases}$$

We further denote \mathbf{W}^{uv} the matrix \mathbf{W} deprived from its uth row and vth column and we remind that the (u, v)-minor of \mathbf{W} is the determinant of this deprived matrix, that is $|\mathbf{W}^{uv}|$.

Theorem 1 (Matrix Tree Theorem Chaiken and Kleitman (1978); Meilă and Jaakkola (2006)). For any symmetric weight matrix W, the sum over all spanning trees of the product of the weights of their edges is equal to any minor of its Laplacian. That is, for any $1 \le u, v \le p$,

$$W := \sum_{T \in \mathcal{T}} \prod_{(j,k) \in T} w_{jk} = |\mathbf{Q}^{uv}|.$$

In the following, without loss of generality, we will choose \mathbf{Q}^{pp} . As an extension of this result, Meilă and Jaakkola (2006) provide a close form expression for the derivative of W with respect to each entry of \mathbf{W} .

Lemma 1 (Meilă and Jaakkola (2006)). Define the entries of the symmetric matrix M as

$$[\mathbf{M}]_{jk} = \begin{cases} \left[(\mathbf{Q}^{pp})^{-1} \right]_{jj} + \left[(\mathbf{Q}^{pp})^{-1} \right]_{kk} - 2 \left[(\mathbf{Q}^{pp})^{-1} \right]_{jk} & 1 \le j < k < p \\ \left[(\mathbf{Q}^{pp})^{-1} \right]_{jj} & k = p, 1 \le j \le p \\ 0 & 1 \le j = k \le p. \end{cases}$$

it holds that

$$\partial_{w_{jk}}W = [\mathbf{M}]_{jk} \times W.$$

B Supplement

B.1 Simulation results

	n < 50	$n \ge 50$	p < 20	$p \ge 20$
EMtree	0.41 (0.11)	0.6 (0.15)	0.38 (0.12)	0.71 (0.21)
gCoda	0.12(0.47)	0.07 (0.03)	0.05 (0.03)	0.09(0.06)
SpiecEasi	2.41 (0.25)	2.41 (0.25)	2.39 (0.25)	2.42 (0.25)

Table 4: Median and standard-deviation of running times for each method in seconds, for n and p parameters. corresponding to Erdös and cluster structures with 5/p densities.

B.2 Illustrations

B.2.1 Fatala River fishes

Species names with highest betweenness scores: 13: Galeoides decadactylus; 19: Liza grandisquamis, 22: Pseudotolithus brachygnatus, 25: Pellonula leonensis, 27: Polydactylus quadrifilis, 30: Pseudotolithus typus, 32: Tylochromis intermedius.

B.2.2 Oak tree mildew

	EMtree neighbors	Jakuschkin et al. (2016)	
OTUs	Putative species/ genus/ Taxonomic classification in RDP (confidence %)	Neighbor	Significant*
B11	Bacteroidetes (100 %), Cytophagales (100 %), Hymenobacter (97 %)		X
B1191	Hymenobacter sp.	X	X
B20	$Methylobacterium\ sp.$	x	X
B29	Alphaproteobacteria (87 %), Rhizobiales (87 %), Methylobacterium (84 %)		X
B304	Alphaproteobacteria (88 %)		X
B31	Sphingomonas sp.	X	X
B444	$Methylobacterium\ sp.$	x	X
F19	Fungi (99 %)	x	X
F26	Taphrina carpini	x	X
F28	Sporobolomyces gracilis	x	X
F29	NA		
F3	Ascomycota (80 %)		X
F32	NA		
F579	NA		
F63	NA		

Table 5: OTUs identified as neighbors of Ea by EMtree (90% selection threshold): comparison with Jakuschkin et al. (2016) (*: significantly associated with infected samples).